Journal of FISH BIOLOGY

fsbi An International Society for Fish Biology

Journal of Fish Biology (2015) **86**, 845–853
doi:10.1111/jfb.12605, available online at wileyonlinelibrary.com

Vertical habitat shift of viviparous and oviparous deep-sea cusk eels revealed by otolith microstructure and stable-isotope composition

N. N. Chang*, E. Y. Liu*, Y. C. Liao† and J. C. Shiao*‡

**Institute of Oceanography, National Taiwan University, 1, Sec. 4, Roosevelt Rd, Taipei, Taiwan, Republic of China and †National Museum of Marine Science and Technology, No. 367, Pei-Ning Rd., Zhongzheng Dist., Keelung City, Taiwan, Republic of China*

(Received 22 July 2014, Accepted 12 November 2014)

Otolith stable-oxygen-isotope composition and microstructure were analysed in order to investigate the vertical habitat shift of deep-sea cusk eels (Ophidiiformes). Otolith δ^{18}O profiles suggested that both viviparous blind cusk eels and oviparous cusk eels experienced a pelagic larval stage and then settled to the deep-sea floor over a vertical distance that ranged among individuals from 200 to >1000 m. This result shows that the larvae of viviparous *Barathronus maculatus* undertake an ontogenetic vertical migration after a period of larval drift that may facilitate their wide distribution on the sea floor.

Key words: *Barathronus maculatus*; ontogenetic vertical migration; Ophidiidae; oxygen isotope; vertical distribution.

Distributions of benthic deep-sea fishes on the sea floor are dependent on their reproductive strategies and ontogenetic vertical migration during their early life stages. Ophidiiformes (cusk eels) are common in deep-sea environments and have different reproductive strategies (*e.g.* oviparous and viviparous) among families. Most ophidiids are oviparous and the larval fishes are hatched in the pelagic zone (Fahay, 1992), yet fishes belonging to the Aphyonidae (blind cusk eels) and Bythitidae give birth to young fishes directly (Nielsen *et al.*, 1999). Larval and juvenile viviparous cusk eels are believed to inhabit adult living depths and undertake little vertical migration throughout their life (Nielsen *et al.*, 1999). A juvenile *Barathronus pacificus* Nielsen & Eagle 1974 of 41·8 mm total length, L_T, was collected from waters shallower than 260 m in the Tasman Sea (Okiyama & Kato, 1997). The adults, however, generally inhabit depths from 3334 to 3860 m. This finding implies a possible pelagic larval stage for aphyonids, particularly those of the genus *Barathronus*, but the data were still insufficient to verify the migratory life history of deep-sea cusk eels.

The otolith stable-oxygen-isotope composition coupled with microstructure analysis can reconstruct the historical residence depths of fishes. The microstructures of otoliths

---

‡Author to whom correspondence should be addressed. Tel.: +886 2 33663227; email: jcshiao@ntu.edu.tw

TABLE I. Biological and sampling information of the cusk eels (Ophidiiformes) used for the analysis of otolith oxygen isotope composition

Family; species	Code	Depth (m)	Date	Station	Location	M (g)	L_T (cm)
Ophidiidae (oviparous)							
Dicrolene tristis	DT1	673	November 2012	SWT1	22° 23′ N; 120° 70′ E	22	16·7
	DT2	673	November 2012	SWT1		16	15·4
Monomitopus pallidus	MP1	850	November 2012	SWT2	22° 14′ N; 120° 16′ E	60	21·9
	MP2	850	November 2012	SWT2		75	22·1
	MP3	673	November 2012	SWT1	22° 23′ N; 120° 70′ E	39	18·9
M. kumae	MK1	850	November 2012	SWT2	22° 14′ N; 120° 16′ E	62	21·7
	MK2	850	November 2012	SWT2		32	19·2
	MK3	850	November 2012	SWT2		6	11·2
Aphyonidae (viviparous)							
Barathronus maculatus	BM1	1228	June 2005	NET1	24° 24′ N; 122° 13′ E	95	21·3
	BM2	1224	June 2005	NET1	24° 23′ N; 122° 14′ E	57	20·1
	BM3	1440	March 2008	P1	13° 34′ N; 120° 48′ E	–	–

L_T, total length; M, mass.

can reveal important life-history events, such as hatching, settlement and metamorphosis (Hislop *et al.*, 2001; Plaza *et al.*, 2001; Hirakawa *et al.*, 2007). Moreover, otolith chemical composition such as otolith $\delta^{18}O$ ($\delta^{18}O_{oto}$), which is in equilibrium with ambient water and affected by salinity, temperature and water $\delta^{18}O$ ($\delta^{18}O_w$) values (Kalish, 1991; Campana, 1999) records a time series of environmental signals. Previous studies demonstrated linearly negative correlations between $\delta^{18}O_{oto}$ and ambient water temperature (Grossman & Ku, 1986; Høie *et al.*, 2004). Thus, they can be used to track fish movement along a temperature gradient, *e.g.* depth (Shephard *et al.*, 2007). The goal of this study was to uncover the residence depths of both oviparous and viviparous cusk eels and reconstruct their habitat use throughout their life history.

For investigating residence depths of cusk eels with different reproductive strategies, three species belonging to the oviparous Ophidiidae: *Dicrolene tristis* Smith & Radcliffe 1913 ($n = 2$), *Monomitopus pallidus* Smith & Radcliffe 1913 ($n = 3$) and *Monomitopus kumae* Jordan & Hubbs 1925 ($n = 3$), and one species of viviparous Aphyonidae: *Barathronus maculatus* Shcherbachev 1976 ($n = 3$) were collected from deep-sea areas around Taiwan and the Philippines (Table I and Fig. 1). Most fish samples were collected on the R.V. *Ocean Researcher I* with a bottom beam trawl but three alcohol-preserved *B. maculatus* (BM1, BM2 and BM3) were provided by the Biodiversity Research Museum, Academia Sinica, Taiwan.

The sagittal otoliths of these fishes were extracted and ground along the sagittal plane until the primordium was exposed. Sub-samples (*c.* 40 μg) of otolith powders were collected sequentially from the edge to the core with intervals of *c.* 55–160 μm using a micromill (ESI; http://www.esi.com/) [see Lin *et al.* (2012) for the sampling details]. The tip of the drill was *c.* 200 μm in diameter (H23RS, Comet; www.kometdental.de) and the drilling depth was set at 50 μm. The milled powders

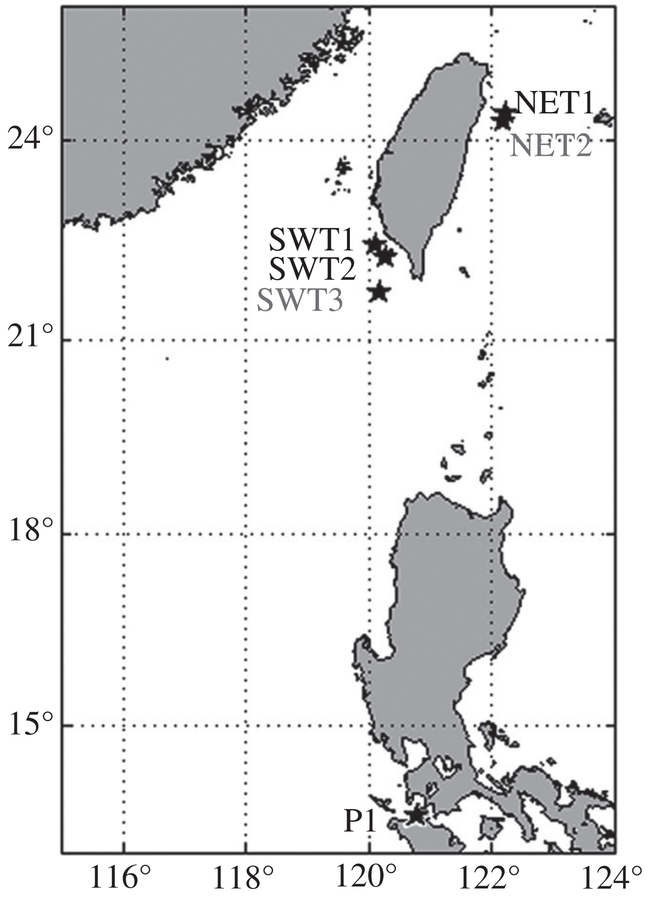

Fig. 1. The cusk eels (Ophidiiformes) were collected around Taiwan (NET1, SWT1-2) and the Philippines (P1). Hydrographical data were measured at NET2 and SWT3.

were allowed to react with pure orthophosphoric acid at 70° C in an automated online system (Kiel Carbonate IV; www.thermoscientific.com) to evolve CO_2 gas that was further analysed by a mass spectrometer (Finnigan MAT 253; Thermo Electron Corporation; www.thermoscientific.com) for oxygen isotopic composition. The long-term reproducibility of the Finnigan MAT 253 is better than ±0·08‰ for δ^{18}O (one S.D.) based on replicate measurements of NBS19 (*c.* 40 μg) during the experimental period. $\delta^{18}O_{oto}$ values (‰) were reported in standard notation as the following, compared to Vienna Pee Dee Belemnite (VPDB) standards through calibration against the NBS19 standard: $\delta = [(R_{sample}/R_{standard}{}^{-1})] \times 1000$ (‰), where R is the ratio of ^{18}O:^{16}O for the sample and the standard.

Water temperature [Fig. 2(a)] and $\delta^{18}O_w$ [Fig. 3(a)] values were used to predict $\delta^{18}O_{oto}$ [Fig. 3(b)] based on the modified equation from Kim & O'Neil (1997) which is enriched by 0·6‰ in aragonite relative to calcite at 25° C (Grossman & Ku, 1986): $\delta^{18}O_{oto} - \delta^{18}O_w = 3{\cdot}71 - 0{\cdot}206T$, where $\delta^{18}O_{oto}$ and $\delta^{18}O_w$ are the otolith δ^{18}O value (VPDB scale) and water δ^{18}O value (VSMOW scale; Vienna standard mean

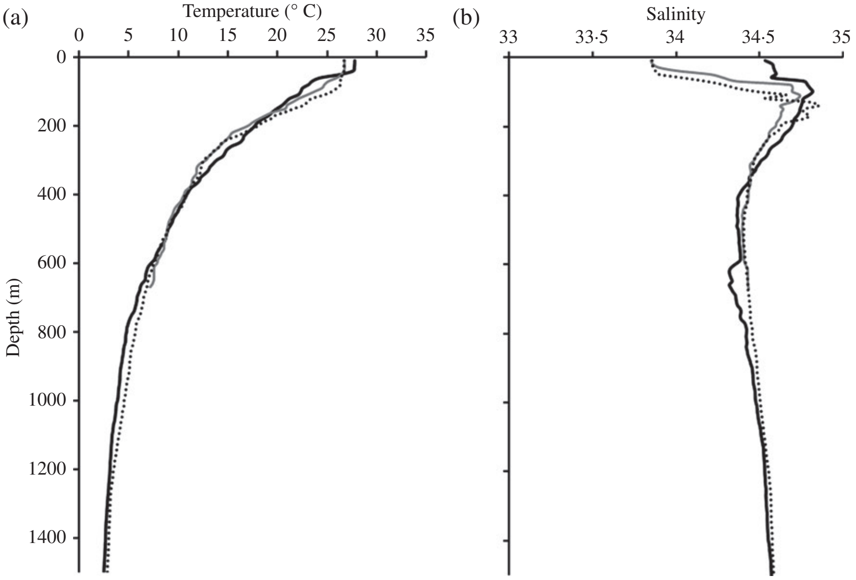

FIG. 2. Hydrological data (a) temperature and (b) salinity measured *in situ* [NET2 (——), SWT2 (——) and SWT3 (……); see Fig. 1] with a SeaBird conductivity–temperature–depth recorder (www.seabird.com). Measurements at NET2 and SWT3 were used to calculate the $\delta^{18}O_w$ and $\delta^{18}O_{oto}$ at the sites NET1 and SWT1, respectively.

ocean water), respectively, and T is the water temperature (° C). The $\delta^{18}O_w$ values (VSMOW) were derived from the measured salinity (S) [Fig. 2(b)] *via* the following equation built with data from the Luzon Strait (Lin, 2000): $\delta^{18}O_w = -13{\cdot}2 + 0{\cdot}39S$. The $\delta^{18}O_w$ values of CO_2 (VSMOW scale) were converted to the VPDB scale. According to Friedman & O'Neil (1977), the fractionation of this conversion equalled 1·00022 and the $\delta^{18}O$ value of CO_2 produced by acid reaction with VPDB calcite is innately higher than the CO_2 equilibrated with VSMOW water by 0·22‰. Thus, the conversion equation can be shown as: $\delta^{18}O_{wVSMOW} = 1{\cdot}00022\delta^{18}O_{wVPDB} + 0{\cdot}22$, *i.e.* $\delta^{18}O_{wVPDB} = 0{\cdot}99978\delta^{18}O_{wVSMOW} - 0{\cdot}22$. Accordingly, the residence depth of the fish can be estimated from the measured $\delta^{18}O_{oto}$ value based on the profile of depth (inferred from temperature) and predicted $\delta^{18}O_{oto}$ [Fig. 3(b)]. The precision of the estimated temperature by $\delta^{18}O_{oto}$ was *c.* ±1° C for single otolith analysis.

From the sea surface to 200 m depth, water temperatures decreased by 8·4–16·2° C [Fig. 2(a)], $\delta^{18}O_w$ values increased from −0·4 to −0·2‰ to 0·05 to 0·11‰ [Fig. 3(a)] and the predicted $\delta^{18}O_{oto}$ values increased by 2·13 to 3·62‰ [Fig. 3(b)] among sampling sites. At depths between 200 and 1500 m, $\delta^{18}O_w$ values changed within a very narrow range [Fig. 3(a)], but temperature decreased by *c.* 15° C [Fig. 2(a)], resulting in a predicted $\delta^{18}O_{oto}$ increase of *c.* 3·1‰ [Fig. 3(b)]. $\delta^{18}O_{oto}$ values mainly reflected the variations in water temperature. A 1‰ raise in $\delta^{18}O_{oto}$ values generally represents about a 4·8° C decrease in water temperature.

Accessory growth centres (AGC), which are reported to be related to habitat changes (Morioka *et al.*, 2001) or larval metamorphosis, existed in all examined cusk eels (Fig. 4). The mean ± S.D. distance from the AGC to otolith core was smaller for

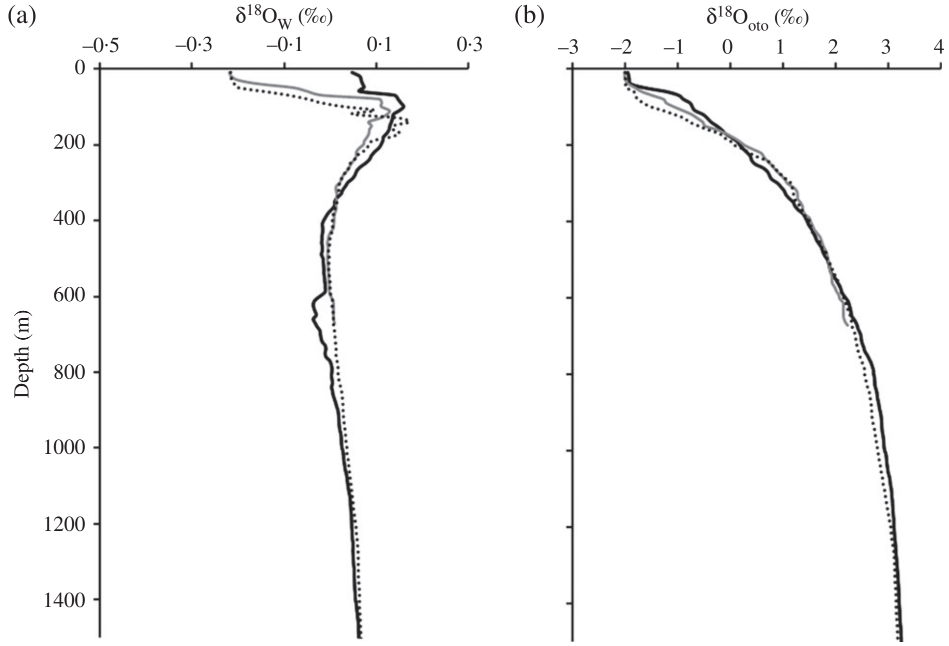

FIG. 3. Vertical profile of (a) sea water oxygen isotope ratios ($\delta^{18}O_w$) estimated from (b) salinity and otolith oxygen isotope ratios ($\delta^{18}O_{oto}$) predicted from water temperature and $\delta^{18}O_w$ [NET2 (——), SWT2 (——) and SWT3 (……); see Fig. 1]. Both $\delta^{18}O_w$ and $\delta^{18}O_{oto}$ are in the Vienna Pee Dee Belemnite (VPDB) scale.

B. maculatus (88·1 ± 18·4 μm) than for *M. pallidus* (168·8 ± 7·9 μm), *M. kumae* (164·0 ± 23·7 μm) and *D. tristis* (149·7 ± 12·7 μm), yet there was no significant difference among these three species ($P > 0{\cdot}05$, $\chi^2 = 6{\cdot}98$; Kruskal–Wallis test). This may imply an earlier habitat change for the viviparous *B. maculatus*. The mean ± S.D. number of increments between core and the AGC was highest for *D. tristis* (21·0 ± 2·6) and lower for *B. maculatus* (19·3 ± 1·5) and *M. pallidus* (17·6 ± 2·3). The width of growth increments sharply decreased from the AGCs to the first translucent zone (TZ; Fig. 4). The distance between first TZ and core varied in the range of 237–986 μm and it was significantly smaller for *D. tristis* than for other species ($P < 0{\cdot}01$, $\chi^2 = 5{\cdot}94$; Kruskal–Wallis test). The first TZ commonly occurs in the otolith of fishes with a pelagic larval stage (Wilson & McCormick, 1999) and may be deposited during bottom settlement, such as for the greater fork-beard *Phycis blennoides* (Brünnich 1768) (Casas & Piñeiro, 2000), greeneye *Chlorophthalmus albatrossis* Jordan & Starks 1904 (Hirakawa *et al.*, 2007) and some grenadiers (Macrouronidae) (Lin *et al.*, 2012).

The $\delta^{18}O_{oto}$ values rapidly increased from the core to the first TZ and then remained steady (variation <0·5‰) beyond the first TZ in *B. maculatus*, *M. pallidus* and *M. kumae*. $\delta^{18}O_{oto}$ values for *B. maculatus* generally increased from 2·11 to 2·38‰ at the core region to 2·99 to 3·59‰ near the first TZ [Fig. 5(a)], corresponding to a depth shift from 560 to 690 m to 1050 to 1500 m. Only the individual BM3 exhibited a great drop in $\delta^{18}O_{oto}$ values to 1·28‰ at around 300–400 μm prior to the subsequent increase. This may reflect a rapid shift in habitat from the adult living depth to shallower water

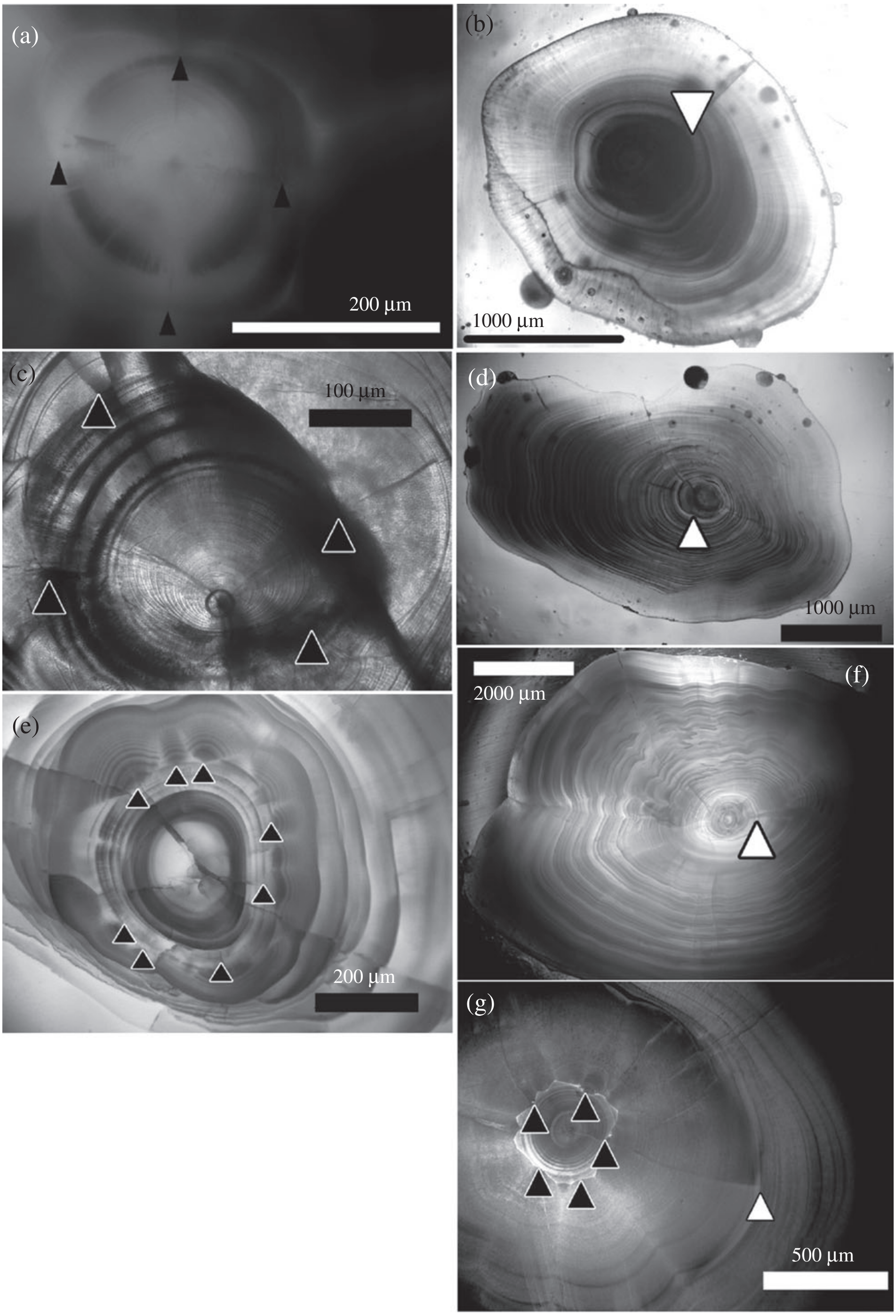

Fig. 4. Otolith microstructure of accessory growth centres (▲) and the first translucent zone (△). (a, b) *Barathronus maculatus*, (c, d) *Dicrolene tristis*, (e, f) *Monomitopus pallidus* and (g) *Monomitopus kumae*.

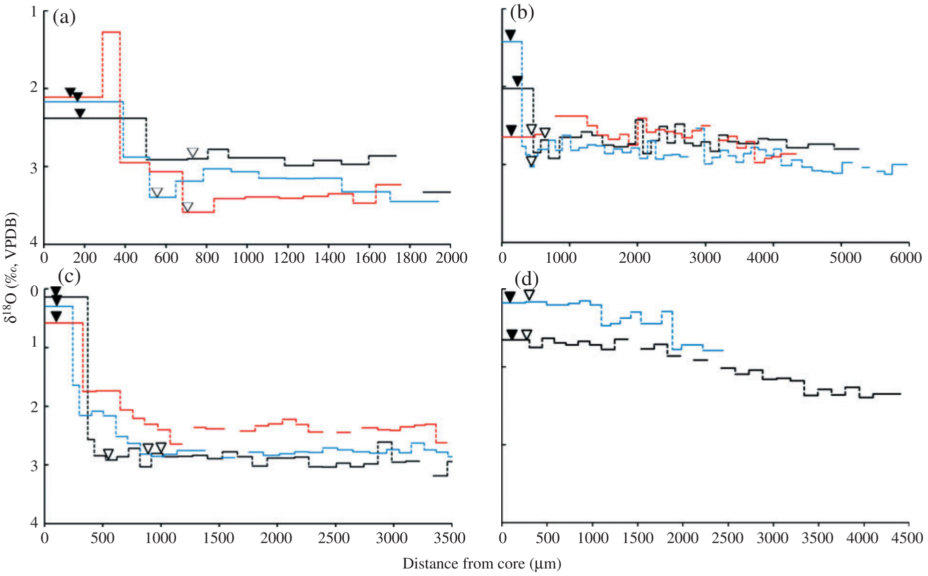

FIG. 5. The $\delta^{18}O_{oto}$ Vienna Pee Dee Belemnite (VPDB) profiles of the cusk eels: (a) *Barathronus maculatus* [three fish: BM1 (——), BM2 (——) and BM3 (——)], (b) *Monomitopus pallidus*[three fish: MP1 (——), MP2 (——) and MP3 (——)], (c) *Monomitopus kumae* [three fish: MK1 (——), MK2 (——) and MK3 (——)] and (d) *Dicrolene tristis*[two fish: DT1 (——) and DT2 (——)]. The positions of accessory growth centres (▼) and the first translucent zone (▽) are indicated

column during the early life stage. For *M. pallidus*, $\delta^{18}O_{oto}$ values increased from 1·30 to 2·48‰ at the core to 2·45 to 2·85‰ at the first TZ [Fig. 5(b)], representing a depth shift from *c*. 360 to 550 m in the larval stage to near 1100 m during the benthic stage. $\delta^{18}O_{oto}$ values of *M. kumae* dramatically increased from 0·14 to 0·58‰ to a plateau of 2·21–2·86‰ [Fig. 5(c)], indicating a depth shift from 210 to 240 m to 850 to 1030 m. The $\delta^{18}O_{oto}$ values of *D. tristis*, however, showed little change between the core and the adjoining first TZ. Instead, $\delta^{18}O_{oto}$ values of *D. tristis* gradually increased from 1300 μm to the otolith edge [Fig. 5(d)] and the estimated depths only changed slightly from *c*. 260 to 320 m in the larval stage to 480 to 690 m at the benthic stage. The major peak of $\delta^{18}O_{oto}$ values at the first TZ confirmed that the first TZ was deposited at the settlement of the cusk eels, except for *D. tristis*.

The otolith is a three-dimensional structure with fast growth along the anterior-posterior axis and slow accretion along the distal-proximal direction (Shiao *et al.*, 2005). Each sub-sample collected by the micromill contained $CaCO_3$ across many layers of the otolith, representing different accreting periods. Thus, the shift in $\delta^{18}O_{oto}$ values (and in depth) might be obscured and the highest and lowest signals might be diluted by the integrated powders (Hanson *et al.*, 2010). Compared with the conventional drilling method, secondary ion mass spectrometry (SIMS) can provide higher temporal and spatial resolution due to the small ion-beam size. Shiao *et al.* (2014) analysed the $\delta^{18}O_{oto}$ profile for one *B. maculatus* by SIMS and found a dramatic increase in $\delta^{18}O_{oto}$ between 642 and 830 μm from the core, indicating a rapid habitat shift from the pelagic to the benthic environment. This transient change was too brief to be detected by the mechanical drilling and IRMS analysis. The $\delta^{18}O_{oto}$ profile of *B. maculatus* analysed by the SIMS, however, reached a plateau of *c*. 6·6‰, which was higher than the predicted values shown in Fig. 3(b). In contrast, the measured $\delta^{18}O_{oto}$ peaks (2·99–3·59‰) for *B. maculatus* by IRMS in this study were consistent with the predicted values.

In conclusion, these results suggest that both oviparous ophidiids and viviparous *B. maculatus* undertook a habitat shift from a shallower habitat to the deep-sea floor with the migratory distance differing among ontogenetic stages. A pelagic early life stage might facilitate the wide dispersal of pelagic larvae *via* current drift and consequently of adults on the deep-sea floor.

We thank Wang Pei-Ling and Taiwan MOST Geochemical Services Platform for assisting in isotope analysis, and B. Jessop for useful suggestions to this manuscript. This research was funded by the Ministry of Science and Technology of Taiwan (MOST 103-2611-M-002-001).

References

Campana, S. E. (1999). Chemistry and composition of fish otoliths: pathways, mechanisms and applications. *Marine Ecology Progress Series* **188,** 263–297.

Casas, J. M. & Piñeiro, C. (2000). Growth and age estimation of greater fork-beard (*Phycis blennoides* Brünnich 1768) in the north and northwest of the Iberian Peninsula (ICES Division VIIIc and IXa). *Fisheries Research* **47,** 19–25.

Fahay, M. P. (1992). Development and distribution of cusk eel eggs and larvae in the middle Atlantic Bight with a description of *Ophidion robinsi* n. sp. (Teleostei: Ophidiidae). *Copeia* **1992,** 799–819.

Friedman, I. & O'Neil, J. R. (1977). Compilation of stable isotope fractionation factors of geochemical interest. In *Data of Geochemistry*, 6th edn (Fleischer, M. & Chap, K. K, eds), pp. 1–12. *Geological Survey Professional Paper* (*United States*) **440**.

Grossman, E. L. & Ku, T. L. (1986). Oxygen and carbon isotope fractionation in biogenic aragonite: temperature effects. *Chemical Geology* **59,** 59–74.

Hanson, N. N., Wurster, C. M., EIMF & Todd, C. D. (2010). Comparison of secondary ion mass spectrometry and micromilling/continuous flow isotope ratio mass spectrometry techniques used to acquire intra-otolith $\delta^{18}O$ values of wild Atlantic salmon (*Salmo salar*). *Rapid Communications in Mass Spectrometry* **24,** 2491–2498.

Hirakawa, N., Suzuki, N., Narimatsu, Y., Saruwatari, T. & Ohno, A. (2007). The spawning and settlement season of *Chlorophthalmus albatrossis* along the Pacific coast of Japan. *Raffles Bulletin of Zoology Supplement* **14,** 151–154.

Hislop, J. R., Gallego, A., Heath, M. R., Kennedy, F. M., Reeves, S. A. & Wright, P. J. (2001). A synthesis of the early life history of the anglerfish, *Lophius piscatorius* (Linnaeus 1758) in northern British water. *ICES Journal of Marine Science* **58,** 70–86.

Høie, H., Andersson, C., Folkvord, A. & Karlsen, O. (2004). Precision and accuracy of stable isotope signals in otoliths of pre-reared cod (*Gadus morhua*) when sampled with a high-resolution micromill. *Marine Biology* **144,** 1039–1049.

Kalish, J. M. (1991). ^{13}C and ^{18}O isotopic disequilibria in fish otoliths: metabolic and kinetic effects. *Marine Ecology Progress Series* **75,** 191–203.

Kim, S. T. & O'Neil, J. R. (1997). Equilibrium and nonequilibrium oxygen isotope effects in synthetic carbonates. *Geochimica et Cosmochimica Acta* **61,** 3461–3475.

Lin, C. F. (2000). Oxygen isotope compositions of seawaters from the South China Sea and Luzon Strait. MS Thesis, National Sun Yat-sen University, China. Available at http://ndltd.ncl.edu.tw/cgi-bin/gs32/gsweb.cgi?o=dnclcdr&s=id=%22088NSYS5271005%22.&searchmode=basic/

Lin, H. Y., Shiao, J. C., Chen, Y. G. & Iizuka, Y. (2012). Ontogenetic vertical migration of grenadiers revealed by otolith microstructures and stable isotopic composition. *Deep-Sea Research I* **61,** 123–130.

Morioka, S., Machinandiarena, L. & Villarino, M. F. (2001). Preliminary information on internal structures of otoliths and growth of ling, *Genypterus blacodes* (Ophidiidae), larvae and juveniles collected off Argentine. *Bulletin of the Japanese Society of Fisheries Oceanography* **65,** 59–66.

Nielsen, J. G., Cohen, D. M., Markle, D. F. & Robins, C. R. (1999). FAO Species Catalog, Vol. 18. Ophidiiform fishes of the world (Order Ophidiiformes). An annotated and illustrated catalogue of pearlfishes, cusk-eels, brotulas and other ophidiiform fishes known to date. *FAO Fisheries Synopsis* **125**.

Okiyama, M. & Kato, H. (1997). A pelagic juvenile of *Barathronus pacificus* (Ophidiiformes: Aphyonidae) from the Southwest Pacific, with notes on its metamorphosis. *Ichthyological Research* **44,** 222–226.

Plaza, G., Katayama, S. & Omori, M. (2001). Otolith microstructure of the black rockfish *Sebastes inermis*. *Marine Biology* **139,** 797–805.

Shephard, S., Trueman, C., Rickaby, R. & Rogan, E. (2007). Juvenile life history of NE Atlantic orange roughy from otolith stable isotopes. *Deep-Sea Research I* **54,** 1221–1230.

Shiao, J. C., Lin, L. Y., Horng, J. L., Hwang, P. P. & Kaneko, T. (2005). How can teleostean inner ear hair cells maintain the proper association with the accreting otolith? *Journal of Comparative Neurology* **488,** 331–341.

Shiao, J. C., Itoh, S., Yurimoto, H., Iizuka, Y. & Liao, Y. C. (2014). Oxygen isotopic distribution along the otolith growth axis by secondary ion mass spectrometry: applications for studying ontogenetic change in the depth inhabited by deep-sea fishes. *Deep-Sea Research I* **84,** 50–58.

Wilson, D. T. & McCormick, M. I. (1999). Microstructure of settlement-marks in the otoliths of tropical reef fishes. *Marine Biology* **134,** 29–41.